

A Simplified Approach for Estimating Skin Permeation Parameters from *In Vitro* Finite Dose Absorption Studies

PAUL A. LEHMAN

QPS, LLC, Delaware Technology Park, Newark, Delaware 19811

Received 19 June 2014; revised 3 September 2014; accepted 3 September 2014

Published online in Wiley Online Library (wileyonlinelibrary.com). DOI 10.1002/jps.24189

ABSTRACT: Historically, percutaneous absorption permeation parameters have been derived from *in vitro* infinite dose studies, yet there is uncertainty in their accuracy if the applied vehicle saturates or damages the *stratum corneum*, or when the permeation parameters are inappropriately derived from cumulative absorption data. An approach is provided for determining penetration parameters from *in vitro* finite dose data. Key variables, and equations for their derivation, are identified from the literature and provide permeation parameters that use only T_{\max} , AUC, and AUMC from finite dose data. The equations are tested with computer-generated model data and to actual study data. Derived permeation parameters obtained from the computer model data match those used in generating the simulated finite dose data. Parameters obtained from actual study data reasonably and acceptably model the penetration profile kinetics of the study data. From *in vitro* finite dose absorption data, three parameters can be obtained: the diffusion transit time (t_d), which characterizes the diffusion coefficient, the partition volume ($V_m P$), which characterizes the partition coefficient, and the permeation coefficient (K_p). These parameters can be obtained from finite dose data without having to know the length of the diffusion pathway through the membrane. © 2014 Wiley Periodicals, Inc. and the American Pharmacists Association J Pharm Sci

Keywords: percutaneous absorption; finite dose; permeation parameters; *in vitro* models; skin; diffusion; pharmacokinetics; mathematical models

INTRODUCTION

The kinetic profiling of *in vitro* infinite dose steady-state percutaneous absorption has been most often characterized by Fick's Laws of diffusion^{1–3} as shown in Eqs. (1–4).

$$J_{ss} = \frac{PDC}{l} \quad (1)$$

$$K_p = \frac{PD}{l} \quad (2)$$

$$J_{ss} = K_p C \quad (3)$$

$$T_{lag} = \frac{l^2}{6D} \quad (4)$$

where J is flux, P is the partition coefficient, D is the diffusion coefficient, C is the concentration of drug in the donor phase (assuming infinite sink in the receptor phase), l is the diffusional pathway length, and K_p is the permeability constant.

When cumulative absorption (often used in the vernacular as “cumulative penetration”) from an infinite dose study is plotted, the slope of the asymptotic linear portion of the curve represents the steady-state flux (dQ/dt), and its x -axis intercept, the lag time (T_{lag}). From T_{lag} and J_{ss} (see Table 1 for variable

definitions), and a measured or estimated length of the diffusion pathway (e.g., *stratum corneum* thickness), a diffusion coefficient and partition coefficient can be derived.

Franz,^{4,5} publishing on the relevance of the *in vitro* finite dose model, also demonstrated the influence of each permeation coefficient on the shape of the kinetic absorption profile. At that time, the finite dose model was defined as being applicable when the applied dose is considered clinically relevant (e.g., 1–10 mg/cm²) and where the kinetic absorption profile demonstrates a depletion of the applied dose over time. This model has become a widely recognized method^{6,7} as it better represents the actual exposure one encounters in the use of cosmetics and topical pharmaceuticals. One solution of the finite dose model is shown in Eq. (5) from Carslaw and Jaeger.⁸

$$J = 2hpDC_0 \sum_{n=1}^{\infty} \frac{\alpha_n e^{-D\alpha_n^2 t}}{\sin \alpha_n l [l(\alpha_n^2 + h^2) + h]} \quad (5)$$

where v is vehicle dose layer thickness, $h = \frac{v}{l}$, and α_n = roots of $[al \tan \alpha l] = hl$.

What is so often misunderstood in consideration of infinite and finite dose data analysis is that a small donor volume (applied dose) does not *a priori* define it to be a finite dose, and conversely, a large donor volume does not *a priori* define it to be an infinite dose. To be a finite dose, it must demonstrate dose depletion kinetics resulting from absorption, volatilization, or precipitation of the solute of interest. To be an infinite dose, it must maintain a constant concentration of diffusible solute in the applied vehicle to sustain a steady-state flux. Further, a clinically relevant dose does not *a priori* define it to be a finite dose. Though many clinically relevant dose applications do result in a finite dose delivery profile, Figure 1 demonstrates two examples from the author's files that show an infinite

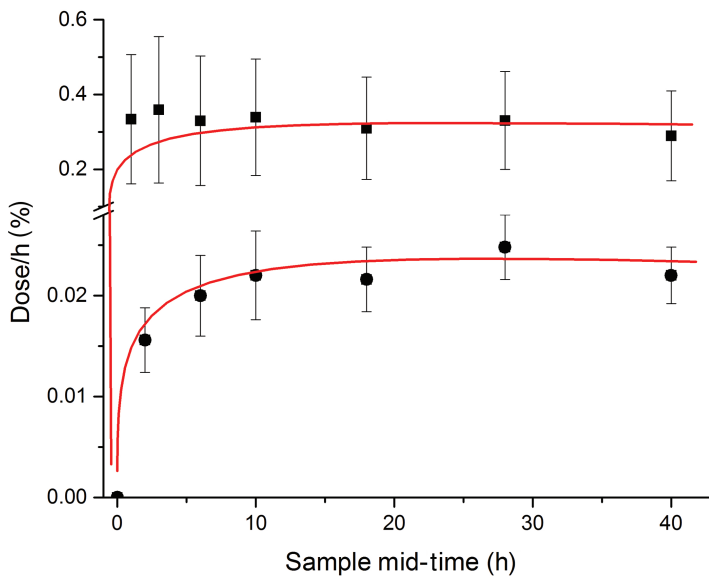
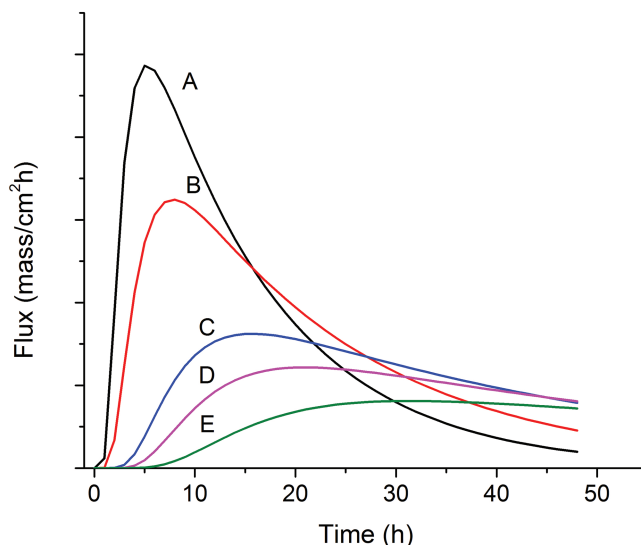
Correspondence to: Paul A. Lehman (Telephone: +253-447-8932; E-mail: paul.lehman@QPS.com)

Journal of Pharmaceutical Sciences

© 2014 Wiley Periodicals, Inc. and the American Pharmacists Association

Table 1. Variables Used in the Equations and Text with Brief Definitions

Variable	Units	Description
A_m	cm^2	Area of the membrane
AUC_{0-t}	Mass/cm^2	Area under the flux curve; $t = 0$ to $t = \text{last}$
$AUMC_{0-t}$	$\text{Mass}\text{-time}/\text{cm}^2$	Area under the flux first moment curve; $t = 0$ to $t = \text{last}$
$AUC_{0-\infty}$	Mass/cm^2	Area under the flux curve; $t = 0$ to $t = \text{infinity}$
$AUMC_{0-\infty}$	$\text{Mass}\text{-time}/\text{cm}^2$	Area under the flux first moment curve; $t = 0$ to $t = \text{infinity}$
C	Mass/cm^3	Concentration
D	cm^2/h	Diffusion coefficient
Dose	Mass	Amount applied. $AUC_{0-\infty}$ for finite dose model
J_{max}	$\text{Mass}/\text{cm}^2/\text{time}$	Peak observed flux
J_{ss}	$\text{Mass}/\text{cm}^2/\text{time}$	Steady-state flux
K_p	cm/h	Permeability coefficient
l	cm	Diffusional pathway or <i>stratum corneum</i> thickness
MTT	h	Mean transit time
P	–	Partition coefficient (membrane to vehicle)
t_d	h	Diffusion transit time
T_{max}	h	Time of peak flux
v	cm	Donor vehicle thickness
V_d	cm^3	Volume of donor vehicle
V_m	cm^3	Volume of membrane
V_mP	cm^3	Partitioning volume
V_{dN}	–	Donor volume number

**Figure 1.** Apparent steady-state absorption from a clinically relevant applied dose ($5 \mu\text{L}/\text{cm}^2$) on dermatomed human skin *in vitro* (mean \pm SE, $n = 6$ donors each in triplicate). (■) 5% minoxidil from a commercial aerosol formulation, and (●) 5% imiquimod from a commercial cream formulation. Solid lines represent estimated fit of the data.**Figure 2.** Computer-generated finite dose flux profiles, 0–48 h, generated using Eq. (5).

dose steady-state absorption profile from a small applied dose volume.

The use of the infinite dose study design for determining permeation coefficients of solutes has proven problematic as the *stratum corneum* is often damaged, saturated, or modified by the continuous exposure to the dosing vehicle. Derived diffusion parameters are less likely a characteristic of the permeating compound but more likely a representation of its diffusion through a vehicle-modified membrane.⁹ This issue is of lesser concern for finite dose studies as the applied volume of vehicle is typically very small and often contain volatile excipients that evaporate rapidly (such as water and alcohol). As a result, the potential for damage or alteration to the *stratum corneum* barrier is appreciably reduced, negligible, or inconsequential. More importantly, any change that is induced to the membrane by the vehicle or its excipients would be clinically relevant, such as would be intended from a penetration enhancer.

Data from *in vitro* absorption studies are frequently presented as cumulative absorption, which is then used to derive K_p and T_{lag} values. However, without also analyzing the data as flux versus time, the true nature of the actual kinetic profile may not be realized. To demonstrate this, a series of finite dose modeled flux curves were generated using Eq. (5). As seen in Figure 2, each curve demonstrates a finite dose absorption profile with a rise to a peak flux (J_{max}), as penetration increases, followed by a decline in flux as the applied vehicle is depleted of the permeating compound.

If this were a study that was terminated at 12, 24 (Fig. 3), 36, or 48 h and profiled only as cumulative absorption versus time, one would falsely interpret the results as demonstrating steady-state flux because of a visualized asymptotic linearity to the data. Even through 48 h, curves D and E would still suggest a steady-state rate of absorption when in fact the finite dose flux profile is a broad curve with a protracted T_{max} .

The consequence of relying only on cumulative absorption to calculate K_p , when in fact the data represent a finite dose absorption profile is demonstrated in Table 2. Permeation

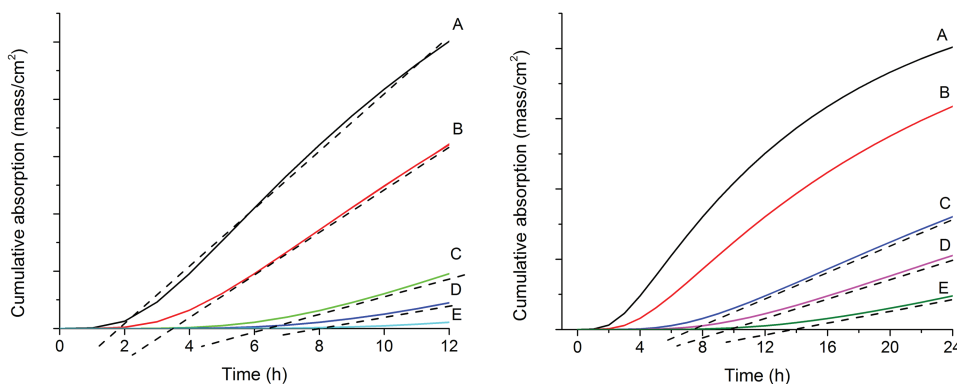


Figure 3. Cumulative absorption (left: 0–12 h; right: 0–24 h). Solid lines from the data of Figure 2. Dashed lines suggest the asymptotic linear portion from the data.

Table 2. Permeability Coefficient ($K_p \times 10^{-6}$ cm/h) as Determined from the Slope of the Apparent Asymptotic Linear Portion of the Cumulative Penetration Curves Shown in Figure 3 (Using Eq. (3))

Curve	0–12 h	0–24 h	0–36 h	0–48 h	True K_p
A	5.11	–	–	–	61.7
B	3.77	–	–	–	41.1
C	1.61	1.89	–	–	20.6
D	0.93	1.42	1.38	–	15.4
E	0.30	0.83	0.97	0.95	10.3

Empty cells represent where positive x -axis intercepts (T_{lag}) could not be defined (<0 h). True K_p values were obtained from Eq. (2) using the D , P , and l values that generated the curves.

coefficients were calculated from the slope of the apparent linear portion of the cumulative absorption curves (Fig. 3) when the x -axis intercept (interpreted as T_{lag}) was more than 0 h. True K_p was determined using Eq. (2) from the initial values for D , P , and l used to generate the curves in Figure 2. One can see the magnitude in K_p error when cumulative absorption curves are misinterpreted as if indicating that J_{ss} had been achieved.

Two examples,^{10,11} observed in peer reviewed literature, are used here to demonstrate the misapplication of cumulative absorption data to characterize *in vitro* absorption. In both examples, an assumed infinite dose volume, containing different solutes, were applied to *ex vivo* skin for the purpose of comparing vehicle effects on absorption. J_{ss} and K_p values were calculated from the data and reported. The data, reproduced from the publications, are shown in Figures 4a and 5a as cumulative absorption. In the adjoining graphs, the same data were converted to flux versus time by this author. Figure 4b demonstrates that steady-state flux was never achieved and the data show a finite dose profile. Figure 5b demonstrates one formulation with a finite dose profile, and the second formulation having yet to demonstrate a peak rate of absorption or a steady-state rate of absorption. Both examples illustrate how cumulative absorption data can mislead an investigator into an incorrect estimation of J_{ss} and K_p .

Historically, K_p has been used as the collective parameter to characterize a solute's percutaneous absorption from steady-state data. Unfortunately, no simple mathematical approach has become available to analyze nonsteady-state permeation data and, therefore, no simple way to calculate K_p from finite

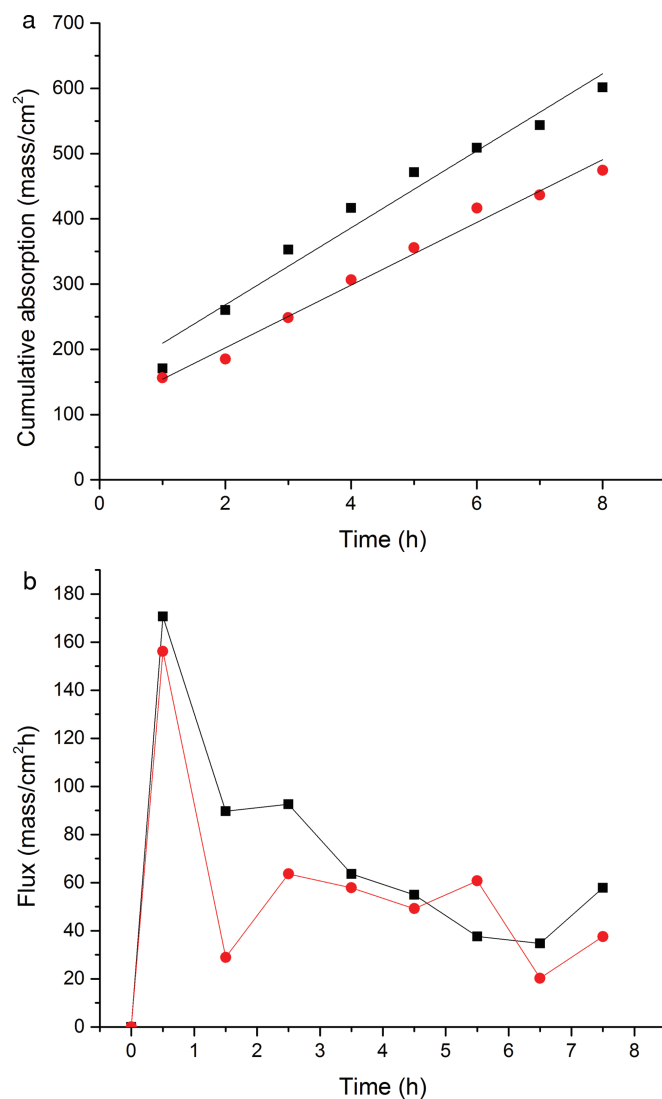


Figure 4. An example data set comparing two formulations on the absorption of a pharmaceutical ingredient from a 100 μ L dose. (a) Cumulative absorption redrawn from the graph shown in the journal article. Lines represent the linear regression of the data that were used to estimate J_{ss} and K_p by the original authors. (b) Data recalculated as Flux. ■, Formulation #1; ●, Formulation #2. Reproduced from Özgüney et al.¹⁰ with permission from AAPS.

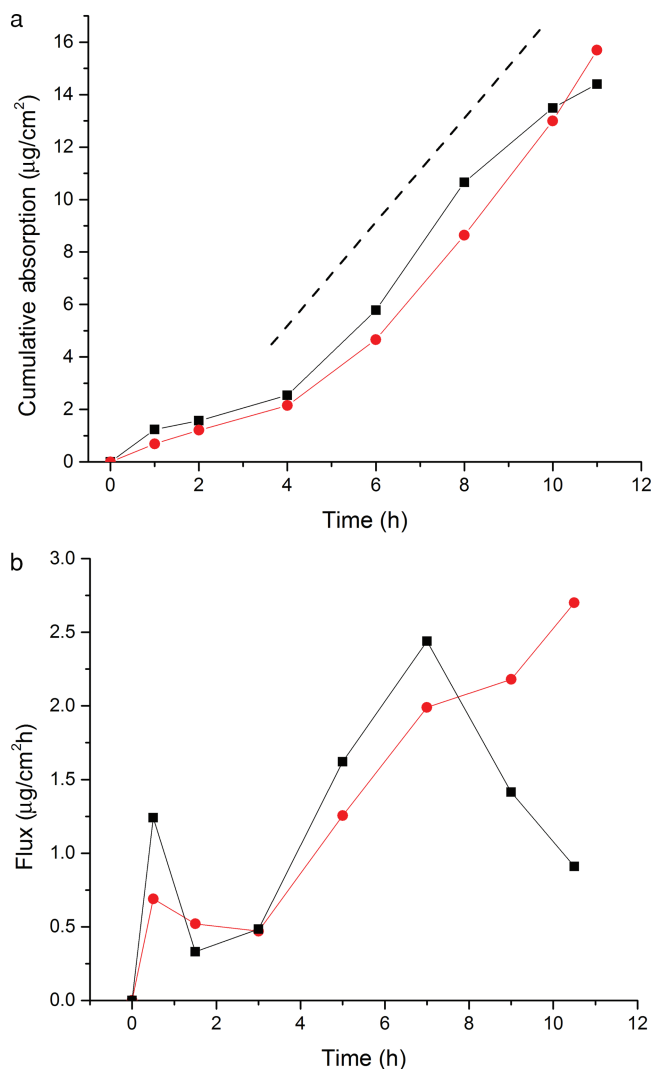


Figure 5. An example data set comparing two formulations on the absorption of a pharmaceutical ingredient from a 1 g dose. (a) Cumulative absorption using the tabulated mean data provided in the journal article. Dashed line demarcates the portion of the curve that was used to estimate J_{ss} and K_p by the original authors. (b) Data recalculated as flux. ■, Formulation #1, ●, Formulation #2. Reproduced from Akhtar et al.¹¹ with permission from Bioline International.

dose studies. With the difficulties posed when using infinite dose applications and cumulative absorption data, the goal of this work was to determine whether useful permeation parameters, and a permeability coefficient, could be obtained from finite dose studies using flux versus time data.

In the literature, there has evolved an extensive and varied mathematical characterization and modeling of percutaneous absorption.^{12–15} It was found that the work provided by Anissimov and Roberts,¹⁶ using methods of Laplace transformations, may yield useful arithmetic derivations that could be applied to *in vitro* finite dose data. From their publication, two parameters were identified for evaluation: t_d , representing diffusion transit time (note Table 3 with equations identified with letters), and V_mP , representing partition volume (V_m , membrane volume; P , partition coefficient). The potential usefulness of these two parameters is that they are easily derived from finite dose data, provide constructive information about the diffusion

and partition coefficients related to the membrane and vehicle, and do not require knowing the travel distance of the solute's diffusional pathway through the membrane.

METHODS

This evaluation will assume the simplest diffusion model: an *in vitro* study that would be conducted with a well-stirred donor volume showing depletion of the solute over time, the receptor under the skin being a perfect sink, and the viable epidermis and dermis offering no resistance to diffusion or binding of the solute. It is appreciated that these assumptions may be overly generous for vehicles that consist predominately or exclusively of volatile excipients, and for complex solutes that may have extreme or unusual absorption characteristics, for which this permeation parameter derivation approach may not necessarily apply.

Computer-generated modeling was conducted using a computer program written in Microsoft Basic language by Dr. Cliff Patlak. Input parameters consist of dose, vehicle thickness, P , D , and l . From this information, the program generates a tabulation of time versus flux based on the finite dose solution using the Carslaw and Jaeger equation (Eq. (5)).

To accomplish this examination, the *in vitro* study needs to have data collected to clearly identify T_{max} and J_{max} , the receptor sampling following T_{max} must be of sufficient duration to obtain AUC_{0-t} , $AUMC_{0-t}$, and where the logarithmic linearity of the terminal declining flux curve can be characterized. Equations in Table 3 were used to test the model derived finite dose flux curves (Fig. 2), and published study data, to determine their suitability to derive t_d , V_mP , D , P , and K_p . The derived parameters were then tested for their ability to correctly profile the absorption data using Eq. (5).

The partition volume (V_mP) was determined by first calculating mean transit time (MTT) from the finite dose data using Eq. E with $AUMC_{0-\infty}$ and $AUC_{0-\infty}$, which was then used in Eq. G to obtain V_{dN} , which, with Eq. F, and V_d , provides V_mP .

The diffusion transit time (t_d) was determined using Eqs. B–D, which, based on the author's assessments, are interchangeable, and each will provide the same end value. These three equations only differ in which two of three variables are being used (T_{max} , V_{dN} , or MTT).

The diffusion coefficient (D) was determined using Eq. A, rearranged to isolate D , and an estimated diffusion pathway length. The partition coefficient (P) was determined using Eq. F, rearranged to isolate P , and an estimated membrane volume.

The first test of the equations in Table 3 was performed using the computer-generated model data shown in Figure 2. Assuming these curves were from an actual study, the equations presented in Table 3 were used to obtain t_d , V_mP , D , and P from the flux data and compared with the initial parameters used to generate the curves with the computer.

The second evaluation of the equations was conducted on actual study data. Four sets of data were retrieved from prior presented work to test their ability to estimate permeation parameters. These studies had been conducted using a standardized *in vitro* study design protocol developed in the author's laboratory. The studies used *ex vivo* dermatomed human skin, or full thickness rat skin, mounted on static Franz diffusion cells with a finite applied dose (e.g., 5–10 μL). Example 1 is a subset of the study data in which the percutaneous absorption of 5%

Table 3. Equations Discussed in the Text

Eq. ID	Expression	Description	Eq. # in Ref.16
A	$t_d = \frac{l^2}{D}$	Diffusion transit time	#19
B	$t_d = \frac{6T_{\max}}{(1 + \frac{2V_{dN}}{V_m})}$	Diffusion transit time	Rearrangement of #53
C	$t_d = MTT \left(2 - \frac{8}{1 + \sqrt{9 + \frac{24}{\frac{MTT}{T_{\max}} - 3}}} \right)$	Diffusion transit time	Rearrangement of #61
D	$t_d = \frac{MTT}{(\frac{1}{2} + V_{dN})}$	Diffusion transit time	Not numbered
E	$MTT = \frac{\int_0^{\infty} tJ(t)dt}{\int_0^{\infty} J(t)dt}$ or $MTT = \frac{AUMC_{0-inf}}{AUC_{0-inf}}$	MTT, Mean Transit Time. The ratio of the area under the first moment curve to the area under the curve for the log-flux versus time curve	#57
F	$V_mP = \frac{V_d}{V_{dN}}$	V_mP , partition volume	Rearrangement of #18
G	$\frac{1}{V_{dN}} = \sqrt{\frac{9}{4} + \frac{6}{\frac{MTT}{T_{\max}} - 3}} - \frac{3}{2}$	V_{dN} , donor volume number	Rearrangement of #62

All obtained from Ref.16.

tetracaine in a vehicle containing ethanol and water (curve B) was compared with a vehicle consisting of 50:50 ethanol–dimethyl sulfoxide (curve A) in human skin (poster presentation: AAPS 2002 Annual Meeting; data on file). Example 2 is a subset of the study data in which percutaneous absorption of 5% lidocaine was evaluated in *ex vivo* skin from control Fischer rats (curve A) and diabetic rats (curve B).¹⁷ Example 3 is a subset of the study data in which the percutaneous absorption of 15% Azelaic acid from a gel formulation, with a moisturizer lotion pretreatment (curve A), compared with no pretreatment (curve B) in human skin.¹⁸ Example 4 is a subset of the study data in which the percutaneous absorption of caffeine and testosterone were each evaluated separately in a neat petrolatum vehicle in human skin.¹⁹

From each data set, t_d , V_mP , D , and P were determined as previously described. The parameters obtained were then fed into the software program for Eq. (5) to determine whether those calculated parameters would model the original data. Goodness of fit between the actual data and the model fit were evaluated using the Pearson product–moment correlation coefficient and the coefficient of determination.

RESULTS

The first test was performed using the model data shown in Figure 2. To conserve space, only the results from curves A and C are shown in Table 4 as the same conclusion was found from all five curves. These results indicate that the data-derived parameters, using the equations in Table 3, match the original parameters that were used to generate the data in Figure 2.

The second evaluation was conducted on the four sets of actual study example data previously described. The parameters obtained are shown in Table 5. The data-derived parameters were fed into Eq. (5) to generate model curves, which are shown overlaid onto the original data in Figures 6–9.

In the determination of the parameters from the data, it was found that P and D were most influenced by the characterization of T_{\max} and the estimated diffusion pathway length. Table 6 demonstrates the mean percent difference that would be seen from the P and D values shown in Table 5 when the T_{\max} may

Table 4. Permeation Parameters Derived from the Data Presented in Figure 1 for Curves A and C

Source	Curve	V_mP (cm ³)	P	t_d (h)	D (cm ² /h)
True values	A	1.75×10^{-3}	1.00	28.36	1.08×10^{-7}
Using Eq. F from Table 3	A	1.75×10^{-3}	1.00	–	–
Using Eqs. B–D from Table 3	A	–	–	28.36	1.08×10^{-7}
True values	C	1.75×10^{-3}	1.00	85.07	0.36×10^{-7}
Using Eq. F from Table 3	C	1.75×10^{-3}	1.00	–	–
Using Eqs. B–D from Table 3	C	–	–	85.07	0.36×10^{-7}

V_d , 0.0001 cm³; V_m , 0.00175 cm³; P , 1.0; dosing area, 1 cm². True values are based on the original parameters that were used to generate the curves in Figure 2.

have been poorly characterized from actual by ± 15 and ± 30 min, or the diffusion pathway under or overestimated by $\pm 10\%$ and $\pm 20\%$. The impact of a $\pm 10\%$ variance in P and D from this assessment are shown in the computer-generated model results overlaid onto two of the study examples, as shown in Figure 10.

DISCUSSION

Despite the appreciation of the experimental difference between finite and infinite *in vitro* percutaneous absorption study designs, it is frequently observed that cumulative absorption is the sole presentation of the data. This approach recurrently results in the false conclusion that steady-state flux was achieved based on a perceived linearity in the terminal portion of the cumulative absorption curve. Representing the data as flux versus time will, even if simply from a visual standpoint, make it effortless to confirm or refute the presumption of steady-state kinetics. The customary approach for the derivation of K_p values, when falsely assumed steady-state flux profiles are used, will result in erroneous conclusions on the kinetics of the penetrating compound.

Table 5. Permeation Parameters Derived from the Equations in Table 3 for Each Example Data Set Shown in Figures 6–9

Examples	t_d (h)	V_mP (cm ³)	D (cm ² /h)	P	PPMCC	CD
Tetracaine curve A ^a	7.66	1.21×10^{-3}	2.94×10^{-7}	0.81	0.8319	0.4233
Tetracaine curve B ^a	19.77	0.29×10^{-3}	1.14×10^{-7}	0.19	0.9941	0.9795
Lidocaine curve A ¹⁷	7.24	0.35×10^{-3}	2.33×10^{-7}	0.27	0.9917	0.9819
Lidocaine curve B ¹⁷	23.16	1.12×10^{-3}	0.73×10^{-7}	0.86	0.9749	0.8686
Azelaic acid curve A ¹⁸	8.86	1.88×10^{-3}	2.54×10^{-7}	1.25	0.9219	0.8675
Azelaic acid curve B ¹⁸	7.86	1.10×10^{-3}	2.86×10^{-7}	0.73	0.9811	0.9719
Caffeine in petrolatum ¹⁹	22.43	98.89×10^{-3}	1.00×10^{-7}	65.92	0.9738	0.9370
Testosterone in petrolatum ¹⁹	27.62	28.07×10^{-3}	0.82×10^{-7}	18.71	0.9788	0.9645

^aPoster presentation: AAPS 2002 Annual Meeting, data on file.

D and P were determined using the diffusional pathway and membrane volume as indicated in the figure legends.

Goodness of fit is demonstrated using Pearson product–moment correlation coefficient (PPMCC) and coefficient of determination (CD).

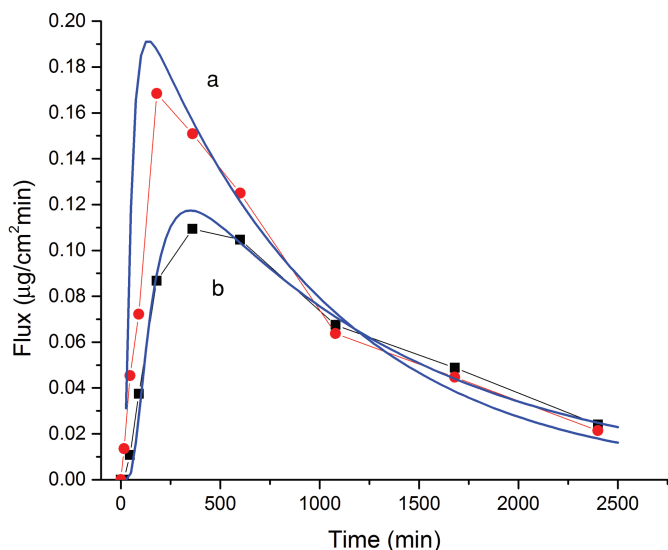


Figure 6. *In vitro* percutaneous absorption of 5% tetracaine in (a) vehicle with dimethyl sulfoxide (DMSO) and (b) vehicle without DMSO. Solid lines are the model-fit results using the diffusion and partition coefficients derived from the data [l assumed to be 0.0015 cm, (a) $V_d = 0.0002$ cm³; (b) $V_d = 0.0025$ cm³].

The objective of this investigation was to determine whether reasonable and useful permeation parameters could be easily derived from finite dose data using the least complicated finite dose model as previously described. Rather than using the more common approach of trial and error estimations of permeation parameters in equations that represent percutaneous absorption to find those parameters that would model the data, the process used here was to derive the permeation parameters t_d , V_mP , D , and P from the actual data, and then to test those parameters with the Carslaw and Jaeger Eq. (5) to determine whether they would model the data. Even with less than ideal data sets, as seen in the examples, a *post hoc* analysis provided parameters that did reasonably model the observed flux profiles as shown in Figures 6–9.

The permeation parameters obtained (t_d and V_mP) from this simple approach can provide different perspectives and information from finite dose study data depending on the intent of the study design. For example, when studying the influence of different vehicles on delivery of a single solute, in most cases,

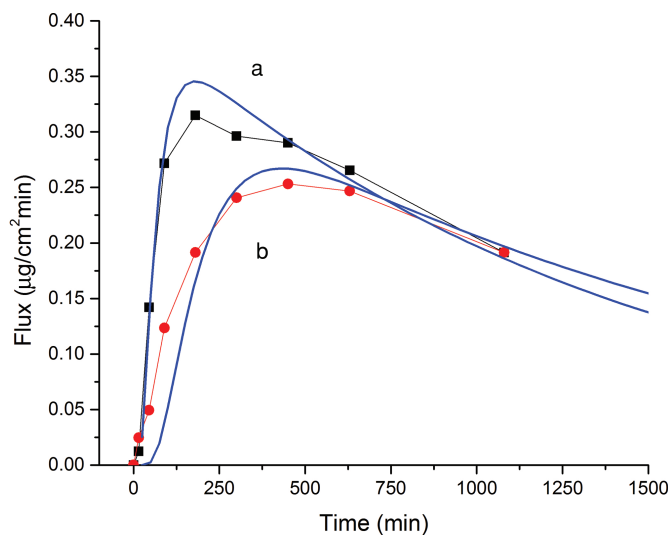


Figure 7. *In vitro* percutaneous absorption of 5% lidocaine in a simple vehicle, in skin from control Fischer rats (a) and diabetic rats (b). Solid lines are the model-fit results using the diffusion and partition coefficients derived from the data (l estimated to be 0.0013 cm, $V_d = 0.0010$ cm³).

one would expect that t_d would not vary, but V_mP would, illustrating the changes in the partition coefficient associated to the thermodynamic influence of each vehicle. When evaluating different solutes in a common vehicle, changes in either or both t_d and V_mP would characterize the chemical structure relationships on partitioning between the vehicle and membrane (V_mP), and/or solute diffusion through the membrane (t_d). For evaluating penetration enhancers, one would expect to see greater differences in t_d , associated to a chemical or physical change in the barrier properties of the membrane associated to the diffusion coefficient, whereas changes in V_mP would represent a vehicle improvement (change in thermodynamic activity) on delivery rather than membrane permeation enhancement.

There is no expectation that all finite dose data can be evaluated for permeation parameters using the described approach, just as there would be no expectation that all percutaneous absorption data can be modeled using the simplest diffusion model, whether as an infinite or finite dose

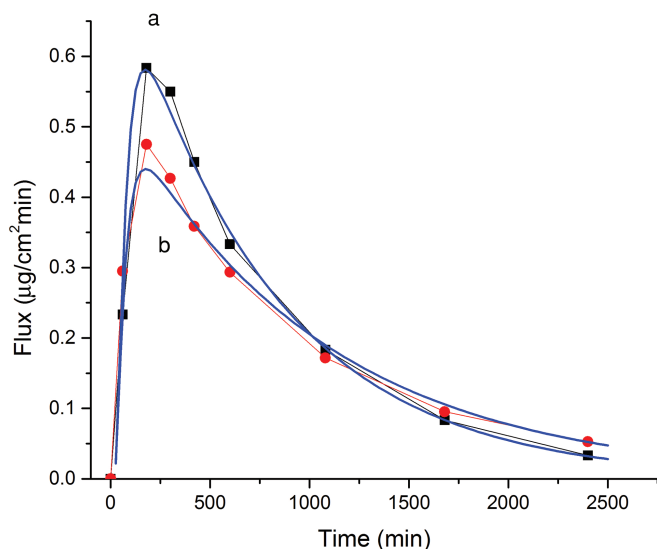


Figure 8. *In vitro* percutaneous absorption of 15% azelaic acid from a gel formulation with a moisturizer lotion pretreatment (a) and without pretreatment (b). Solid lines are the model-fit results using the diffusion and partition coefficients derived from the data (l estimated to be 0.0015 cm, $V_d = 0.0020$ cm³).

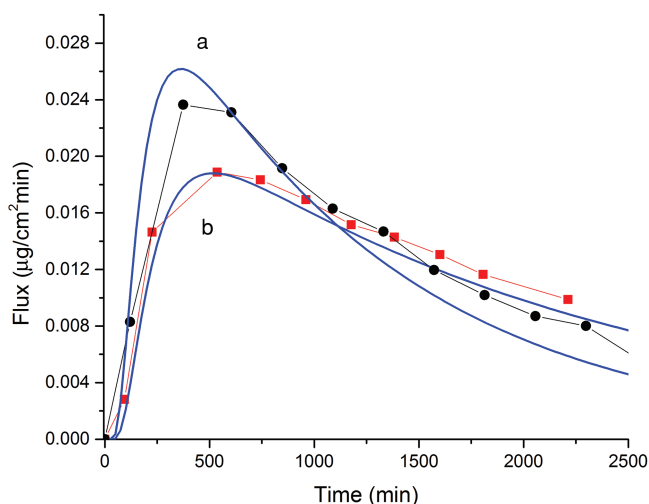


Figure 9. *In vitro* percutaneous absorption of caffeine (a) and testosterone (b), in human skin, each in a neat petrolatum vehicle. Solid lines are the model-fit results using the diffusion and partition coefficients derived from the data (l estimated to be 0.0015 cm, testosterone: $V_d = 0.0250$ cm³; caffeine: $V_d = 0.050$ cm³).

study. However, it was unexpected that the four examples evaluated, selected solely on the basis of having both an identifiable T_{max} , and a practical number of sample points following the T_{max} , to characterize the log-linear decline in flux, could be reasonably modeled using the simplest finite dose model and the parameter derivation method described here.

Not all finite dose absorption profiles can be evaluated using the simplest diffusion model. Three common examples are provided. The first is when the declining flux is not log linear. This may occur when the viable epidermis and dermis are not infinitely permeable, or when there may be the occurrence of

a reservoir or solute binding in the viable epidermis. Though permeation parameters could be derived for separate linear segments of the curve, it may be problematic in their interpretation, or in associating the parameters to represent simple *stratum corneum* permeation.

The second is when steady-state flux is seen from a small dose volume, as shown in Figure 1. This example reaffirms that a small donor volume does not define it to be a finite dose. Even if the studies had continued with a sufficient duration to eventually demonstrate depletion of the applied dose, identification of a T_{max} would be problematic. In this situation, treating the data as if obtained from an infinite dose study design would be a logical option.

The third is when the applied dose is washed from the surface of the skin before an unhindered declining flux phase is observed, negating the ability to obtain the needed AUC and AUMC values. Figure 11 provides an example.¹⁹ However, it is proposed that the decline in solute flux observed following the surface wash may simply represent solute diffusion through the viable epidermis and dermis to the receptor compartment. The solute remaining in the *stratum corneum* would be considered the donor volume and the viable epidermis the membrane. The donor solute content (Dose) would be equivalent to the $AUC_{0-\infty}$ of the flux curve following the surface wash. By using the equations in Table 3, permeation parameters can be obtained. For this example, the epidermal membrane, V_m , was estimated to be 0.0335 cm³ and the *stratum corneum* (the donor compartment), V_d , as 0.0015 cm³. The permeation parameters were found to be: $D = 9.3 \times 10^{-5}$ cm²/h, $P = 2.5 \times 10^{-4}$, $t_d = 0.024$ h, $V_m P = 8.3 \times 10^{-6}$ cm³. It is noteworthy to compare the magnitudes of difference of these values to those derived from the previous examples (Table 5) where the *stratum corneum* is being considered as the primary barrier.

In addition, this simplified approach for the estimation of permeation parameters will not work when the ratio of MTT/T_{max} is ≤ 3.0 . This has been observed from short pulse dose duration studies, and when the vehicle or permeant is highly volatile, particularly when the rate of absorption is influenced by the rate of evaporation, which results in a prolongation of T_{max} as a consequence of the duration of exposure. For these situations, one is referred to the work by Kasting and colleagues²⁰⁻²² for estimating permeation parameters.

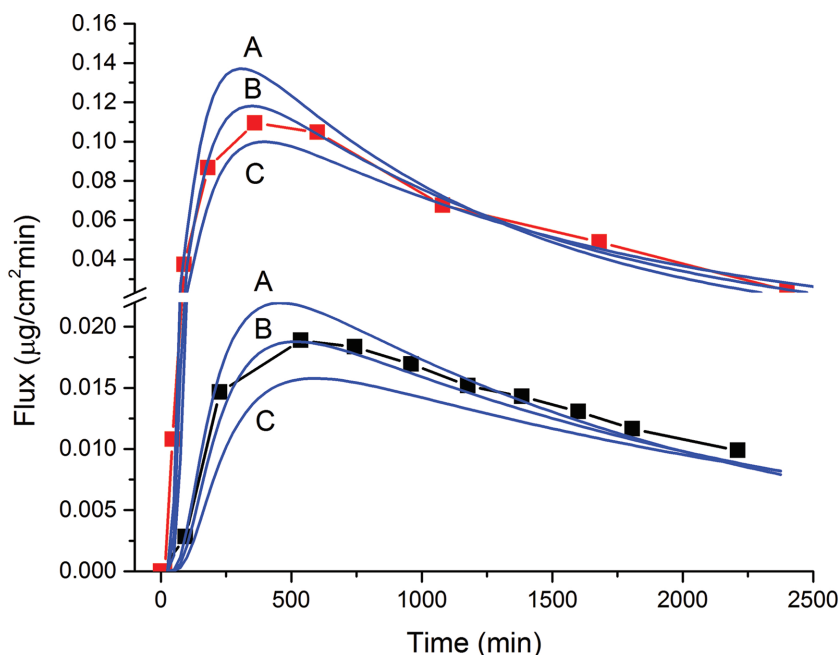
The permeation coefficient (K_p) has been the common element for characterizing and equating percutaneous absorption between studies. However, it has traditionally been obtained from infinite dose studies based on steady-state flux. As previously discussed, the K_p reported may not be representative of the solute or membrane diffusion because of the likely vehicle effects on the barrier, or because of it being incorrectly derived by misapplication of the infinite dose model to nonsteady-state data.

Kubota and Maibach²³ once suggested, using computer simulation, where a K_p value could be derived from an *in vitro* study with a 300–500 μ L applied dose, when the depletion of the solute in the applied dose volume is quantified over time. However, when small donor volumes are used (e.g., 1–10 mg/cm²), this approach would prove problematic. It is proposed here that a permeation coefficient can be obtained from nonsteady-state finite dose data using t_d and V_{dN} . Using Eqs. (6) and (7), when they are multiplied together (Eq. (6)); A_m , area of membrane, rearranged (Eq. (7)), and then inverted (Eq. (8)) a solution for K_p can be defined. Equation (8) can also be expressed as shown in

Table 6. Mean Percent Range Observed for Accuracy of P , D , and K_p when T_{max} or the Diffusion Pathway Length (l) Are Estimated Rather than Actual

Variance from T_{max}	P	D	K_p
-30 min	13.4 to 31.1	-9.8 to -30.7	3.3 to 13.2
-15 min	7.0 to 16.8	-4.8 to -14.2	8.0 to 16.8
+15 min	-7.5 to -21.6	4.5 to 12.2	-7.5 to -1.9
+30 min	-16.0 to -50.4	9.0 to 22.8	-16.0 to -3.8
Variance from Diffusion Pathway Length	P	D	K_p
-20%	-24.5 to -25.3	35.8-36.1	0
-10%	-10.0 to -11.2	18.8-19.1	0
+10%	8.8 to 9.4	-20.8 to -21.1	0
+20%	16.6 to 16.9	-43.6 to -44.2	0

Mean percent range observed across all four data examples in Table 5 when T_{max} was varied by ± 15 and ± 30 min from actual, and the diffusion pathway length was varied $\pm 10\%$ and $\pm 20\%$ from actual.

**Figure 10.** Tetracaine (■; from Fig. 6b) and testosterone (■; from Fig. 9b). Solid blue lines are the model-fit results using the diffusion and partition coefficients derived from the data as shown in Table 5 (curve b), along with +10% P and +10% D (curve a), and -10% P and -10% D (curve c).

Eq. (9) with substitution of V_{dN} from Eq. F with $V_m P$.

$$t_d V_{dN} = \frac{l^2 V_d}{D V_m P} \quad (\text{Where... } V_m = l A_m) \quad (6)$$

$$\frac{t_d V_{dN} A_m}{V_d} = \frac{l}{D P} \quad \left(\text{Where... } K_p = \frac{P D}{l} \right) \quad (7)$$

$$K_p = \frac{V_d}{t_d V_{dN} A_m} \quad \left(\text{Where... } V_m P = \frac{V_d}{V_{dN}} \right) \quad (8)$$

$$K_p = \frac{(V_m P)}{t_d A_m} \quad (9)$$

With t_d having been determined from Eqs. B–D, and V_{dN} from Eq. G, and knowing V_d from the study design, a value for

K_p can be determined from finite dose data. Returning to the computer-generated data shown in Figure 1, Table 7 compares the actual K_p from the D , P , and l values used to generate the curves to the K_p values derived from the flux data analysis using Eq. D. Nominally identical results were found from the data. Using the same process for the example data sets (Figs. 6–9), nonsteady-state K_p values were determined using Eq. (9), and are shown in Table 8.

CONCLUSIONS

The first consideration in evaluating *in vitro* percutaneous absorption data is to establish whether it represents infinite dose or finite dose kinetics, regardless of the intent of the study design or the volume of the vehicle applied to the skin surface. A critical examination of the data will guide the investigator to the appropriate model to calculate permeation parameters. Using the correct model, and its associated permeation parameters, will significantly improve predicting drug delivery,

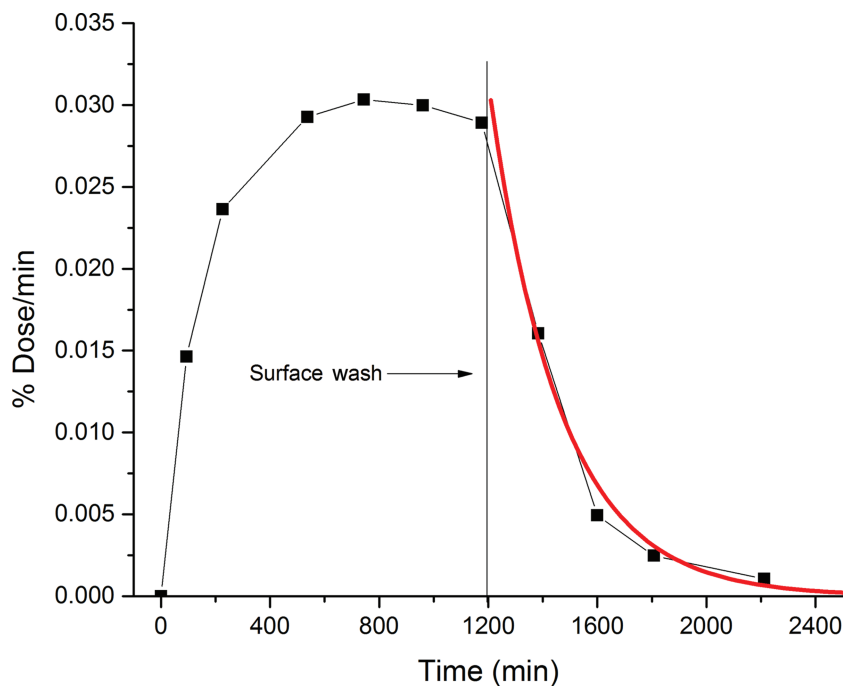


Figure 11. *In vitro* absorption of caffeine, from a water-based gel, with a surface wash at 1200 min.¹⁹ Solid red line is the model-fit results using the diffusion and partition coefficients derived from the data, as described in the text.

Table 7. Determined K_p (cm/h) Values Using Data from Figure 2

Curve	Diffusion Coefficient (cm ² /h)	Initial Parameters using Eq. (2) ($K_p \times 10^{-5}$)	Data Derived from Eqs. B–D from Table 3 and Eq. (9) ($K_p \times 10^{-5}$)
A	1.08×10^{-7}	6.17	6.17
B	0.72×10^{-7}	4.11	4.11
C	0.36×10^{-7}	2.06	2.06
D	0.27×10^{-7}	1.54	1.54
E	0.18×10^{-7}	1.04	1.04

P , 1.0; V_d , 0.0001 cm³; V_m , 0.00175 cm³; dosing area, 1 cm², and with the initial D (cm²/h) values as shown in the table.

Table 8. Apparent K_p Values from the Example Data Sets Shown in Table 5 Using Eq. (9)

Examples	K_p (cm/h)
Tetracaine curve A	1.58×10^{-4}
Tetracaine curve B	0.15×10^{-4}
Lidocaine curve A	4.79×10^{-5}
Lidocaine curve B	4.84×10^{-5}
Azelaic acid curve A	2.12×10^{-4}
Azelaic acid curve B	1.40×10^{-4}
Caffeine in petrolatum	4.41×10^{-3}
Testosterone in petrolatum	1.02×10^{-3}

systemic exposure, as well as assist in a better understanding of the physiological barrier properties of the *stratum corneum*.

Overall, K_p can be retained as a common universal permeation parameter characterizing the complete absorption process, whether obtained from a finite dose or an infinite dose study. However, when derived from a finite dose study, it may better exemplify the penetration and absorption characteris-

tics of the solute unencumbered by the influence that a large vehicle volume may have had on the *stratum corneum* barrier properties. As K_p is a vehicle-dependent parameter, it would be recommended that, when presenting permeation parameters from a finite dose study, t_d and $V_m P$ are also included, as they will contribute to characterizing the diffusion and partition coefficients associated to the solute or vehicle of interest. As the finite dose derivation of K_p has only been shown here as a mathematical construct, it remains to be carefully tested *in vitro* with well-designed studies for confirmation.

ACKNOWLEDGMENT

The author is grateful and indebted to Dr. Thomas Franz and Dr. Sameersingh Raney for our invaluable discussions that led to this publication.

REFERENCES

1. Fick A. 1855. About diffusion. *Phil Mag* 10:30–39.
2. Higuchi T. 1960. Physical chemical analysis of percutaneous absorption process from creams and ointments. *J Soc Cosmet Chem* 11(2):85–97.
3. Scheuplein RJ, Blank IH. 1971. Permeability of the skin. *Physiol Rev* 51:702–747.
4. Franz TJ. 1975. Percutaneous absorption: On the relevance of *in vitro* data. *J Invest Dermatol* 64:190–195.
5. Franz TJ. 1983. The kinetics of cutaneous drug penetration. *Int J Dermatol* 22:499–505.
6. Franz TJ. 1978. The finite dose technique as a valid *in vitro* model for the study of percutaneous absorption in man. *Curr Probl Dermatol* 7:58–68.
7. OECD. 2004b. Test Guideline 428: Skin Absorption: *in vitro* Method. Paris, Organisation for Economic Co-operation and Development.

8. Carslaw HS, Jaeger JC. 1959. Conduction of heat in solids. 2nd ed. London, UK: Oxford University Press, pp 128.
9. Franz TJ, Lehman PA, Franz SF, North-Root H, Demetrulias JL, Kelling CK, Moloney SJ, Gettings SD. 1993. Percutaneous penetration of N-nitrosodiethanolamine through human skin (in vitro): Comparison of finite and infinite dose applications from cosmetic vehicles. *Fundam Appl Toxicol* 21(2):213–221.
10. Özgüney IS, Karasulu HY, Kantarci G, Sözer S, Güneri T, Ertan G. 2006. Transdermal delivery of diclofenac sodium through rat skin from various formulations. *Pharm Sci Tech* 7(4):E1–E7.
11. Akhtar N, Rehman MU, Khan HMS, Rasool F, Saeed T, Murtaza G. 2011. Penetration enhancing effect of polysorbate 20 and 80 on the in vitro percutaneous absorption of L-ascorbic acid. *Trop J Pharm Res* 10(3):281–288.
12. Mitragotri S, Anissimov YG, Bunge AL, Frasch HF, Guy RH, Hadgraft J, Kasting GB, Lane ME, Roberts MS. 2011. Mathematical models of skin permeability: An overview. *Int J Pharm* 418(1):115–129.
13. Anissimov YG, Roberts MS. 2011. Modelling dermal drug distribution after topical application in human. *Pharm Res* 28:2119–2129.
14. Frasch HF, Barbero AM. 2013. Application of numerical methods for diffusion-based modeling of skin permeation. *Adv Drug Deliv Rev* 65:208–220.
15. Kasting GB, Nitsche JM. 2014. Mathematical models of skin permeability: Microscopic transport models and their predictions. In *Computational biophysics of the skin*; Querleux B, Ed. Singapore: Pan Stanford Publishing, pp 187–216.
16. Anissimov YG, Roberts MS. 2001. Diffusion modeling of percutaneous absorption kinetics: 2. Finite vehicle volume and solvent deposited solids. *J Pharm Sci* 90:504–520.
17. Lehman PA. 2014. Effect of induced acute diabetes and insulin therapy on stratum corneum barrier function in rate skin. *Skin Pharmacol Physiol* 27:249-253.
18. Del Rosso JQ, Lehman PA, Raney SG. 2009. Impact of order of application of moisturizers on percutaneous absorption kinetics: Evaluation of sequential application of moisturizer lotions and Azelaic acid gel 15% using a human skin model. *Cutis* 83(3):119–124.
19. Bronaugh RL, Franz TJ. 1986. Vehicle effects on percutaneous absorption: In vivo and in vitro comparisons with human skin. *Brit J Dermatol* 115:1–11.
20. Kasting GB. 2001. Kinetics of finite dose absorption through skin 1. Vanillynonanamide. *J Pharm Sci* 90(2):202–212.
21. Kasting GB, Miller MA. 2006. Kinetics of finite dose absorption through skin 2: Volatile compounds. *J Pharm Sci* 95(2):268–280.
22. Miller MA, Bhatt V, Kasting GB. 2006. Dose and airflow dependence of benzyl alcohol disposition on skin. *J Pharm Sci* 95(2):281–291.
23. Kubota K, Maibach H. 1991. Estimation of the permeability coefficient from a finite-dose, in vitro percutaneous drug permeation study. *J Pharm Sci* 80(10):1001–1002.